Exosomes From 3d Culture of Marrow Stem Cells Enhances Endothelial Cell Proliferation, Migration, and Angiogenesis via Activation of the Hmgb1/akt Pathway

Wenling Gao
Sun Yat-Sen University
Tangzhao Liang
Third Affiliated Hospital of Sun Yat-Sen University
Ronghang He
Third Affiliated Hospital of Sun Yat-Sen University
Jianhua Ren
Third Affiliated Hospital of Sun Yat-Sen University
Hui Yao
Third Affiliated Hospital of Sun Yat-Sen University
Kun Wang
Third Affiliated Hospital of Sun Yat-Sen University
Lei Zhu
Third Affiliated Hospital of Sun Yat-Sen University
Yue Xu (246463354@qq.com)
Sun Yat-Sen University

Research

Keywords: Angiogenesis, bone marrow stem cell, HUVEC, exosome, 3D culture

Posted Date: June 23rd, 2020

DOI: https://doi.org/10.21203/rs.3.rs-37225/v1

Version of Record: A version of this preprint was published at Stem Cell Research on January 1st, 2021.
See the published version at https://doi.org/10.1016/j.scr.2020.102122.

Abstract

BackgroundAngiogenesis is an essential step in tissue engineering. MSCexosomes play an important role in angiogenesis. Functional biomolecules in exosomes vested by the culture microenvironment can be transferred to recipient cells and affects their effect. 3D culture can improve the proliferation and activity of MSCs. However, whether exosomes derived from 3D culture of MSCs have an enhanced effect on angiogenesis is unclear.

MethodsHerein, we compared the bioactivity of exosomes produced by conventional 2D culture (2D-exos) and 3D culture (3D-exos) of bone marrow stem cells (BMSCs) in angiogenesis.

ResultsA series of in vitro and in vivo experiments indicated that 3D-exos exhibited stronger effects on HUVEC cell proliferation, migration, tube formation, and in vivo angiogenesis compared with 2D-exos. Moreover, the superiority of 3D-exos might be attributed to the activation of HMGB1/AKT signaling.

ConclusionsThese results indicate that exosomes from 3D culture of MSCs may serve as a potential therapeutic approach for pro-angiogenesis.

Introduction

Tissue engineering has been recognized as a promising strategy for the treatment of multiple diseases, such as heart disease (1), traumatic diseases (2), as well as bone defects (3). However, insufficient angiogenesis remains a major challenge. Angiogenesis is a complex process of forming new blood vessels from existing ones. It has been reported that interactions between vascular cells and the extracellular environment are important for this process. Currently, cell-based strategies have been increasingly used to promote angiogenesis, including mesenchymal stem cells (MSCs) (4). MSCs are adult multipotent cells that are frequently selected for tissue regeneration because of the excellent capabilities of differentiation to various cell types and promotion of angiogenesis (5-8). In vitro and in vivo studies have demonstrated that MSCs can enhance the proliferation and migration of endothelial cells and accelerate vessel remodeling (9). Nevertheless, accumulating evidence indicates that mesenchymal stem cells exert their effect on angiogenesis through secretion of vesicles such as apoptotic bodies and exosomes, rather than their differentiation capabilities (10).

Exosomes are lipid bilayer membrane-bound vesicles (30 ~ 150 nm) (11), which are secreted by almost all cell types and contain various bioactive proteins, lipids, and RNAs (12). After being endocytosed by recipient cells, exosomes regulate target cell function by transferring RNAs or proteins (10). It has been reported that injection with exosomes derived from human-induced pluripotent stem cell-derived MSCs enhances angiogenesis in the bone repair model (13,14). Similarly, exosomes derived from hypoxia-treated human adipose MSCs also exhibit enhanced effect on angiogenesis, which is mediated by activation of PKA signaling (2). Particular RNA and proteins levels in exosomes can be affected by the microenvironment in which the source cells are maintained. Macroporous scaffolds or fibrous topography have been reported to enhance the paracrine effects of MSCs (15-17), and exosomes

produced from 3D culture of MSCs exhibits improved tissue regeneration activity, as compared with 2D culture (18,19).

Hydroxyapatitescaffolds are artificial devices widely used in tissue engineering(20-22). In this study, BMSCs cultured on hydroxyapatite scaffolds were used as a source to produce exosomes (3D-exos). The effects of 3D-exos on endothelial cell proliferation, migration, tube formation, and in vivo angiogenesis were investigated, and the potential mechanism was also explored.

Materials And Methods

2D and 3D culture of bone marrow stem cells (BMSCs)

BMSCs was purchased from Cyagen Biosciences (Guangzhou, China) and were maintained in Dulbecco's Modifed Eagle's medium (DMEM, Gibco, USA) containing 10 % fetal bovine serum (Life Technologies, Gibco, USA) and 1% penicillin-streptomycin (Gibco, USA). Hydroxyapatite scaffold was 3D-printed as described previously (23). BMSCs were then seeded to the 3D hydroxyapatite scaffolds and cultured at 37°C with 5% CO_2.

Isolation of BMSC-exos

Medium from 3D and 2D culture of BMSCs was collected and used for exosome isolation. Conditioned medium was centrifuged at 3000 g for 15 min and 20,000 g for 45 min. Supernatants were then filtered with a 0.22-μm filter and centrifuged for 70 min at 110,000 g at 4°C to pellet exosomes. The exosomes were washed with PBS and centrifuged for another 70 min at 110,000 g at 4°C.

Transmission electron microscopy

Isolated exosomes were resuspended in PBS. Exosomes were dropped on a copper grid and air-dried. Exosomes were fixed with 3% glutaraldehyde for 2 h and stained with 2% uranyl acetate for 30 s. Then exosomes were visualized under a transmission electron microscope.

Exosome uptake assay

Exosomes were pre-stained with PKH67 using a PKH67 Green Fluorescent Cell Linker Kit (Sigma, USA). Human umbilical vein endothelial cells (HUVECs, 2×10^5/well) were seeded in 6-well plates and 2 μg of PKH67-labeled exosomes was added to the culture. After incubation for 24 h, cells were fixes with 4% paraformaldehyde and DAPI was used to stain the nuclei. The location of exosomes was observed under a confocal microscope (Carl Zeiss, Germany).

Western blot analysis

Exosomes were collected and lysed using RIPA and separated by 12% SDS-PAGE gels for 45 min. Then samples were transferred to PVDF membrane. The membrane was blocked with 5% BSA and incubated

with primary antibodies, such as CD9 (ab59479), CD81 (ab79559), and TSG101 (ab125011), at 4°C overnight. After washing with TBS-Tween, the membrane was incubated with secondary antibody for 1 h at room temperature. The protein bands were detected by chemiluminescence substrate.

Cell counting kit-8 assay

HUVECs (2×10^3 cells/well) were placed in 96-well plates and treated with 10 μg/ml exosomes from 3D or 2D culture of BMSCs. The proliferation of HUVECs was determined using the Cell Counting Kit-8 assay kit (Dojindo Molecular Technologies Inc., Kumamoto, Japan). The absorbance at 450 nm was measured every 24 h. To access the effect of 3D-exos released from scaffolds on cell growth, HUVECs were seeded in 48-well plates containing 3D-exo/hydroxyapatite (3D-exo/HA) scaffolds. After cultured for 1, 3, 7 days, the viability of HUVECs was determined by CCK-8 assay.

Transwell migration assay

The effect of exosome on the migration of HUVEC cells was detected using the Transwell migration assay. HUVECs (1×10^5 cells) in serum-free medium was added into the upper chambers of Transwell (Corning, USA). A total of 5 μg exosomes in 600 μl RPMI-1640 medium containing 1% FBS were added to the lower chamber. After incubating at 37°C for 24 h, HUVECs transferred to the bottom of the insert filter were fixed with methanol and stained with 0.1% crystal violet.

Tube formation assay

Matrigel (300 μl/well) was plated to a 24-well plate and allowed to solidify for 30 min at 37°C. HUVEC cells (1.5×10^4 cells/well) were seeded on top of matrigel and treated with 10 μg/ml exosomes derived from 3D or 2D culture of BMSCs. The number of tubes was counted with three random filed under a light microscope.

Quantitative RT-PCR analysis

After treatment with exosomes (10 μg/ml), total RNA of HUVEC cells was extracted using Trizol reagent (Life science, USA). RNA was transcribed to be cDNA using PrimeScript RT-PCR kit (TaKaRa, Dalian, China). RT-qPCR were performed using SYBR Green (Tiangen Biotech, Beijing, China). The reaction conditions were as follows: 95°C for 3 min, 40 cycles of 95°C for 3 s, 60°C for 30 s. GAPDH was used as an internal control. The relative gene expression was calculated by the $2^{-\Delta\Delta CT}$ method.

DNA plasmid transfection and siRNA interference

The pcDNA3.1-HMGB1 was constructed by Genecopoeia (Guangzhou, China). siRNA targeting HMGB1 and control siRNA were synthesized by Shanghai GenePharma (Hangzhou, China). HUVEC cells were seeded in 6-well plates and grown to 70% (for DNA transfection) or 30~50% confluence (for siRNA transfection). DNA plasmid and siRNA transfections were performed using Lipofectamine 2000.

Release of exosomes from scaffolds

The release rate of exosomes from hydroxyapatite scaffolds was determined by BCA analysis. 3D-exo/HA scaffolds were plated into the 48-well plate with 200 μl PBS. At different time points (3h,6h,12h,24h,48h), the supernatant was collected and 200 μl fresh PBS was added. The exosomes in PBS were counted by BCA analysis.

Animal experiments

After mice were anesthetized with pentobarbital sodium (30 mg/kg), the scaffolds (5 mm in diameter) were subcutaneously implanted into mice to study their angiogenesis. Mice were randomly divided in three groups (n=5), including the control scaffold, 2D-exo scaffolds, and 3D-exo scaffolds. For preparation of 2D-exo/HA scaffolds and 3D-exo/HA scaffolds, the dried scaffolds were incubated in DOPA/Tris-HCl solution for 24 h at 37°C and transferred into 10 μg/ml 2D-exo or 3D-exo PBS solution. After 4 weeks of implantation, scaffold samples were collected and fixed with 4% formaldehyde and embedded in paraffin. The samples were stained by hematoxylin and eosin (HE) and masson, and immunohistochemically stained with anti-VEGF to detect the VEGF expression. Real-time qPCR and Western blotting were also performed to determine the mRNA and protein expression of VEGF and CD31. The animal experiments were approved by XXX.

Statistical analyses

Data were presented as the mean ± SD. Statistical analyses were performed with SPSS 19.0 (SPSS Inc. USA). Comparisons of multiple groups were performed with one-way multivariate analysis of variance (ANOVA) followed by Turkey's test. P value < 0.05 was considered statistically significant.

Results

Characterization of 3D scaffolds and BMSC growth

Hydroxyapatite scaffolds were prepared by 3D printing and the structure were accessed by micro-CT (Fig. 1A). The scaffolds are three-dimensional cylinders with the pore sizes of 200 μm (Fig. 1B). The cell morphology on 2D culture plates and 3D scaffolds were compared. The results showed that BMSCs exhibited a typical spreading morphology on the 2D culture plate, while cells spread on the 3D scaffolds and crossed the interconnected pore walls (Fig. 1C and D).

Characterization of exosomes

Exosomes were isolated from the supernatants of 2D and 3D culture of BMSCs via ultracentrifugation. Analysis by transmission electron microscopy showed that a spherical morphology of 3D-exos and 2D-exos (Fig. 2A). The markers of exosomes, tetraspanins (CD9, CD81) and endosomal pathway protein (TSG101) were detected by Western blotting to characterize the exosomes. The result showed that the expression of CD91, CD81, and TSG101 was highly expressed in 3D-exos than in 2D-exos (Fig. 2B).

Confocal imaging revealed that there were PKH67 fluorescence spots in HUVECs (Fig. 2C), indicating that the HUVECs had an uptake of exosomes.

3D-exos enhance proliferation, migration, and tube formation of HUVECs

At first, the effect of exosomes on HUVEC proliferation was addressed by the CCK-8 assay. Both 2D-exos and 3D-exos could promote the proliferation of HUVEC cells. Moreover, 3D-exos exhibited a much stronger effect on HUVEC proliferation than 2D-exos at 48 h and 72 h (Fig. 3A). Endothelial cell migration and tube formation were important steps of angiogenesis. Thus, we examined the influence of exosomes on the migration and tube formation of HUVEC cells. Transwell migration assay showed that both 2D-exos and 3D-exos could enhance the migration of HUVECs, compared to the control group, but 3D-exos induced a higher migration of HUVECs than 2D-exos (Fig. 3B). In addition, while 2D-exos slightly increased the number of tubes formed by HUVECs, 3D-exos remarkably increased the tube number compared with the control (Fig. 3C). In consistent with this result, the protein and mRNA expression of vascular endothelial growth factor (VEGF) and CD31, two important stimulators implicated in angiogenesis, were significantly increased in both 2D-exo and 3D-exo groups compared with the control group, and the highest expression levels were observed in the 3D-exo group (Fig. 3D and 3E). Together, these results suggest that 3D-exos have a superior ability in HUVEC proliferation, migration, and tube formation than 2D-exos.

3D-exos modulate angiogenesis through HMGB1 and AKT signaling pathway

High mobility group box 1 protein (HMGB1) is a proinflammatory cytokine highly associated with angiogenesis (24,25). Interestingly, while exploring the potential molecules that mediated the enhanced effect of 3D-exos, we observed a significantly upregulation of HMGB1 in 3D-exos compared with 2D-exos. To further verify the critical role of HMGB1 in HUVEC proliferation, migration, and tube formation, loss- and gain-of-function experiments were performed. The results from CCK-8 assay showed that silencing of HMGB1 significantly inhibited the proliferation of HUVECs (Figure 4B), whereas overexpression of HMGB1 enhanced the cell viability (Figure 4B). Similar results were found in Transwell migration assay (Figure 4C) and tube formation assay (Figure S1). Furthermore, the expression levels of p-AKT, VEGF, and CD31 were significantly downregulated following HMGB1 knockdown (Figure 4D). Nevertheless, the expression level of these proteins was increased by HMGB1 overexpression (Figure 4D). Together, these data suggest that 3D-exos exert their function via activation of HMGB1/AKT signaling pathway.

The effect of 3D-exos on angiogenesis in vivo

To determine the effect of exosomes on angiogenesis in vivo, 3D-printed hydroxyapatite scaffolds were coated with dopamine and then incorporated with exosomes (Fig. 5A). As shown in Figure 5B, the exosomes showed burst release from hydroxyapatite scaffolds (Fig. 5B) and 3D-exos released from hydroxyapatite scaffolds showed a higher effect on the proliferative capability of HUVEC that 2D-exos (Fig. 5C). Then, the models of angiogenesis were established by subcutaneous implantation of exosome-containing scaffolds (3D-exo/HA or 2D-exo/HA scaffolds) and exosome-free scaffolds (control) (Fig. 6A).

Histological assessment and masson staining revealed that more blood vessels were found in the tissues from 3D-exo/HA scaffolds compared with those from 2D-exo/HA scaffolds or control scaffolds (Fig. 6B). Immunohistochemical staining also showed that the expression of VEGF was significantly higher in the 3D-exo/HA group than those in the 2D-exo/HA group or the control group (Fig. 6B). Consistently, the mRNA expression of VEGF was markedly increased in 3D-exo/HA group (Fig. 6C). Moreover, higher mRNA and protein expression of CD31, which indicates neo-vessel formation (Fig. 6C and D), were found in the 3D-exo/HA group. Together, these results suggest that 3D-exos promote angiogenesis in vivo.

Discussion

Vascularization is a prerequisite for tissue repair, which provides sufficient blood supply, oxygen, nutrients and growth factors. BMSCs have been reported to play an important role in vascularization, particularly due to their secretion of vesicles (26). Accumulating evidence suggests that exosome is a novel alternative to cell-based approaches due to its superiority in avoiding emboli formation, immunogenicity, and malignant transformation (27).However, the yield and activity of exosomes limit their application. In this study, we found that exosome from 3D scaffold culture of BMSCs had a better yield and greater activities in promoting HUVEC cell proliferation, migration, and angiogenesis compared with those from 2D culture.

Biomaterial scaffolds serve as templates for cell growth and establishment of the vascular system. The properties of scaffolds mainly depend on the nature of the biomaterial. Therefore, biomaterial selection is critical in tissue engineering (28).Hydroxyapatite has been widely used for bone repair, attribute to their simple preparation, low-cost, and the chemical likeness of calcium phosphates to bone mineral (29,30).Compared with 2D plates, 3Dscaffolds offer a porous structure for cell growth and attachment, thus enhancing mechanical connection between the implanted biomaterial and surrounding bone tissue (28). Pu et al. reported that the unique structure of the bilayer scaffolds promotes collagen fiber deposition, cell proliferation, and ingrowth of smooth muscle cells and endothelial cells in vivo (31). Li et al. have also shown that culture in 3D porous scaffolding improves MSC survival by mimicking a microenvironment and promoting a more realistic cellular physiology (32).In this study, we found that BMSCs in 2D culture exhibited a typical spreading morphology while BMSCs in 3D culture established physical contacts with neighboring cells.

Increasing evidence demonstrates that the therapeutic effect of BMSCs is not attributed to multi-lineage function but secreted exosomes, through which proteins, miRNAs and other molecular could be transferred to recipient cells (15,33,34).The 3D scaffolds have been proved to be a key material that modulates the paracrine function of cells (15). Haraszti et al. have reported that 3D-exos show higher yield and improved activity than 2D-exos (35). In present study, we found that 3D-exos of BMSCs had a higher yield, and exerted a more significant effect on HUVEC proliferation, migration, angiogenesis.

HMGB1 is a nonhistone nuclear protein that facilitates the assembly of nucleoprotein complexes and could be passively released or actively secreted to extracellular environment in various diseases including

chronic inflammatory disorders, autoimmune diseases, and cancer (36). Recently, HMGB1 gained more attention as a novel proangiogenic factor that could increase the expression of proangiogenic cytokines VEGF and their receptors(37). HMGB1 has been shown to regulate angiogenesis via vascular endothelial growth factor receptor 2 (VEGFR2) in cholangiocarcinoma (24).In this work, we found that 3D-exos of BMSCs enhanced the angiogenesis by increasing the expression level of HMGB1, VEGF and CD31. Furthermore, PI3K/AKT axis has been reported to be involved in HMGB1-modulated vascularization and invasion (38,39). In line with these results, our data showed that knockdown of HMGB1 reduced the phosphorylation of AKT, whereas overexpression of HMGB1 elevated the level of p-AKT. Taken together, our data suggest that 3D-exos promotes vessel generation through stimulation of HMGB1-AKT signaling.

Conclusion

Our findings showed that 3D-exos generated from BMSCs have superior effects on HUVEC proliferation, migration, angiogenesis than 2D-exos, which is associated with the modulation of HMGB1-AKT signaling. Our results suggest that 3D-exos of BMSCs may serve as a potential therapeutic strategy targeting angiogenesis.

Abbreviations

MSCsmesenchymal stem cells

DMEMDulbecco's Modifed Eagle's medium

HMGB1High mobility group box 1 protein

Declarations

Acknowledgements

We thank all of the members in the lab. We are grateful to the financial support of the National Natural Science Foundation.

Funding

This work was financially supported by the National Natural Science Foundation of China (8180090732)

Authors' contributions

GWLand LTZ designed and performed the experiments, analysed the data and wrote the manuscript. HRH carried out the experiments. RJH and HY performed some of the research. WK helped to review the manuscript. ZL and XY participated in the experimental design, provided financial support and supervised the manuscript. All authors read and approved the final manuscript.

Availability of data and materials

For data availability, please contact the corresponding author.

Ethics approval and consent to participate

All experimental protocols were approved by the Committee of Animal Care and Use at Sun Yat-sen University.

Consent for publication

Not applicable.

Competing interests

There exists no competing interest among the authors.

References

1. Dogan, A., Elcin, A. E., and Elcin, Y. M. (2017) Translational Applications of Tissue Engineering in Cardiovascular Medicine. *Current pharmaceutical design***23**, 903-914
2. Xue, C., Shen, Y., Li, X., Li, B., Zhao, S., Gu, J., Chen, Y., Ma, B., Wei, J., Han, Q., and Zhao, R. C. (2018) Exosomes Derived from Hypoxia-Treated Human Adipose Mesenchymal Stem Cells Enhance Angiogenesis Through the PKA Signaling Pathway. *Stem cells and development***27**, 456-465
3. Shim, J. H., Won, J. Y., Park, J. H., Bae, J. H., Ahn, G., Kim, C. H., Lim, D. H., Cho, D. W., Yun, W. S., Bae, E. B., Jeong, C. M., and Huh, J. B. (2017) Effects of 3D-Printed Polycaprolactone/beta-Tricalcium Phosphate Membranes on Guided Bone Regeneration. *International journal of molecular sciences***18**
4. Geuze, R. E., Wegman, F., Oner, F. C., Dhert, W. J., and Alblas, J. (2009) Influence of endothelial progenitor cells and platelet gel on tissue-engineered bone ectopically in goats. *Tissue Eng Part A***15**, 3669-3677
5. Polymeri, A., Giannobile, W. V., and Kaigler, D. (2016) Bone Marrow Stromal Stem Cells in Tissue Engineering and Regenerative Medicine. *Horm Metab Res***48**, 700-713
6. Kunkel, N., Wagner, A., Gehwolf, R., Heimel, P., Tempfer, H., Korntner, S., Augat, P., Resch, H., Redl, H., Betz, O., Bauer, H. C., and Traweger, A. (2017) Comparing the osteogenic potential of bone marrow and tendon-derived stromal cells to repair a critical-sized defect in the rat femur. *J Tissue Eng Regen Med***11**, 2014-2023
7. Rahbarghazi, R., Nassiri, S. M., Ahmadi, S. H., Mohammadi, E., Rabbani, S., Araghi, A., and Hosseinkhani, H. (2014) Dynamic induction of pro-angiogenic milieu after transplantation of marrow-derived mesenchymal stem cells in experimental myocardial infarction. *International journal of cardiology***173**, 453-466

8. Edwards, S. S., Zavala, G., Prieto, C. P., Elliott, M., Martinez, S., Egana, J. T., Bono, M. R., and Palma, V. (2014) Functional analysis reveals angiogenic potential of human mesenchymal stem cells from Wharton's jelly in dermal regeneration. *Angiogenesis***17**, 851-866
9. Kinnaird, T., Stabile, E., Burnett, M. S., Lee, C. W., Barr, S., Fuchs, S., and Epstein, S. E. (2004) Marrow-derived stromal cells express genes encoding a broad spectrum of arteriogenic cytokines and promote in vitro and in vivo arteriogenesis through paracrine mechanisms. *Circ Res***94**, 678-685
10. Wang, N., Chen, C., Yang, D., Liao, Q., Luo, H., Wang, X., Zhou, F., Yang, X., Yang, J., Zeng, C., and Wang, W. E. (2017) Mesenchymal stem cells-derived extracellular vesicles, via miR-210, improve infarcted cardiac function by promotion of angiogenesis. *Biochimica et biophysica acta. Molecular basis of disease***1863**, 2085-2092
11. Cobelli, N. J., Leong, D. J., and Sun, H. B. (2017) Exosomes: biology, therapeutic potential, and emerging role in musculoskeletal repair and regeneration. *Ann N Y Acad Sci***1410**, 57-67
12. Kourembanas, S. (2015) Exosomes: vehicles of intercellular signaling, biomarkers, and vectors of cell therapy. *Annu Rev Physiol***77**, 13-27
13. Qi, X., Zhang, J., Yuan, H., Xu, Z., Li, Q., Niu, X., Hu, B., Wang, Y., and Li, X. (2016) Exosomes Secreted by Human-Induced Pluripotent Stem Cell-Derived Mesenchymal Stem Cells Repair Critical-Sized Bone Defects through Enhanced Angiogenesis and Osteogenesis in Osteoporotic Rats. *International journal of biological sciences***12**, 836-849
14. Liu, X., Li, Q., Niu, X., Hu, B., Chen, S., Song, W., Ding, J., Zhang, C., and Wang, Y. (2017) Exosomes Secreted from Human-Induced Pluripotent Stem Cell-Derived Mesenchymal Stem Cells Prevent Osteonecrosis of the Femoral Head by Promoting Angiogenesis. *International journal of biological sciences***13**, 232-244
15. Su, N., Gao, P. L., Wang, K., Wang, J. Y., Zhong, Y., and Luo, Y. (2017) Fibrous scaffolds potentiate the paracrine function of mesenchymal stem cells: A new dimension in cell-material interaction. *Biomaterials***141**, 74-85
16. Huang, R., Wang J Fau - Chen, H., Chen H Fau - Shi, X., Shi X Fau - Wang, X., Wang X Fau - Zhu, Y., Zhu Y Fau - Tan, Z., and Tan, Z. (2019) The topography of fibrous scaffolds modulates the paracrine function of Ad-MSCs in the regeneration of skin tissues. *Biomater Sci***7**, 4248-4259
17. Castilla-Casadiego, D. A., Reyes-Ramos, A. M., Domenech, M., and Almodovar, J. A.-O. (2019) Effects of Physical, Chemical, and Biological Stimulus on h-MSC Expansion and Their Functional Characteristics. *Ann Biomed Eng***48**, 519-535
18. Yu, L., Wu, Y., Liu, J., Li, B., Ma, B., Li, Y., Huang, Z., He, Y., Wang, H. A.-O. X., Wu, Z. A.-O., and Qiu, G. (2018) 3D Culture of Bone Marrow-Derived Mesenchymal Stem Cells (BMSCs) Could Improve Bone Regeneration in 3D-Printed Porous Ti6Al4V Scaffolds. *Stem Cells Int*, 2074021
19. Yan, L., and Wu, X. (2020) Exosomes produced from 3D cultures of umbilical cord mesenchymal stem cells in a hollow-fiber bioreactor show improved osteochondral regeneration activity. *Cell Biol Toxicol***36**, 165-178

20. An, S. H., Matsumoto, T., Miyajima, H., Nakahira, A., Kim, K. H., and Imazato, S. (2012) Porous zirconia/hydroxyapatite scaffolds for bone reconstruction. *Dental materials : official publication of the Academy of Dental Materials* **28**, 1221-1231
21. Ozdal-Kurt, F., Tuglu, I., Vatansever, H. S., Tong, S., and Deliloglu-Gurhan, S. I. (2015) The effect of autologous bone marrow stromal cells differentiated on scaffolds for canine tibial bone reconstruction. *Biotechnic & histochemistry : official publication of the Biological Stain Commission* **90**, 516-528
22. Zhu, Y., Li, Z., Zhang, Y., Lan, F., He, J., and Wu, Y. (2020) The essential role of osteoclast-derived exosomes in magnetic nanoparticle-infiltrated hydroxyapatite scaffold modulated osteoblast proliferation in an osteoporosis model. *Nanoscale* **12**, 8720-8726
23. Chen, S., Shi, Y., Zhang, X., and Ma, J. (2020) Evaluation of BMP-2 and VEGF loaded 3D printed hydroxyapatite composite scaffolds with enhanced osteogenic capacity in vitro and in vivo. *Materials science & engineering. C, Materials for biological applications* **112**, 110893
24. Xu, Y. F., Liu, Z. L., Pan, C., Yang, X. Q., Ning, S. L., Liu, H. D., Guo, S., Yu, J. M., and Zhang, Z. L. (2019) HMGB1 correlates with angiogenesis and poor prognosis of perihilar cholangiocarcinoma via elevating VEGFR2 of vessel endothelium. *Oncogene* **38**, 868-880
25. Feng, Y., Ke, J., Cao, P., Deng, M., Li, J., Cai, H., Meng, Q., Li, Y., and Long, X. (2018) HMGB1-induced angiogenesis in perforated disc cells of human temporomandibular joint. *J Cell Mol Med* **22**, 1283-1291
26. Peng J Fau - Chen, L., Chen L Fau - Peng, K., Peng K Fau - Chen, X., Chen X Fau - Wu, J., Wu J Fau - He, Z., He Z Fau - Xiang, Z., and Xiang, Z. (2019) Bone Marrow Mesenchymal Stem Cells and Endothelial Progenitor Cells Co-Culture Enhances Large Segment Bone Defect Repair. *J Biomed Nanotechnol* **15**, 742-755
27. Jia, Y., Zhu, Y., Qiu, S., Xu, J., and Chai, Y. A.-O. (2019) Exosomes secreted by endothelial progenitor cells accelerate bone regeneration during distraction osteogenesis by stimulating angiogenesis. *Stem Cell Res Ther* **10**, 12
28. Nguyen, L. H., Annabi N Fau - Nikkhah, M., Nikkhah M Fau - Bae, H., Bae H Fau - Binan, L., Binan L Fau - Park, S., Park S Fau - Kang, Y., Kang Y Fau - Yang, Y., Yang Y Fau - Khademhosseini, A., and Khademhosseini, A. (2012) Vascularized bone tissue engineering: approaches for potential improvement. *Tissue Eng Part B Rev* **18**, 363-382
29. Wei, G. A.-O., Gong, C., Hu, K., Wang, Y., and Zhang, Y. (2019) Biomimetic Hydroxyapatite on Graphene Supports for Biomedical Applications: A Review. LID - 10.3390/nano9101435 [doi] LID - 1435. *Nanomaterials (Basel)* **9**, 1435
30. Cox, S. C., Thornby, J. A., Gibbons, G. J., Williams, M. A., and Mallick, K. K. (2015) 3D printing of porous hydroxyapatite scaffolds intended for use in bone tissue engineering applications. *Materials science & engineering. C, Materials for biological applications* **47**, 237-247
31. Pu, J., Yuan, F., Li, S., and Komvopoulos, K. (2015) Electrospun bilayer fibrous scaffolds for enhanced cell infiltration and vascularization in vivo. *Acta Biomater* **13**, 131-141

32. Li, X., Wu, A., Han, C., Chen, C., Zhou, T., Zhang, K., Yang, X., Chen, Z., Qin, A., Tian, H., and Zhao, J. (2019) Bone marrow-derived mesenchymal stem cells in three-dimensional co-culture attenuate degeneration of nucleus pulposus cells. *Aging (Albany NY)***11**, 9167-9187
33. Todorova, D., Simoncini, S., Lacroix, R., Sabatier, F., and Dignat-George, F. (2017) Extracellular Vesicles in Angiogenesis. *Circ Res***120**, 1658-1673
34. Cunnane, E. M., Weinbaum, J. S., O'Brien, F. J., and Vorp, D. A. (2018) Future Perspectives on the Role of Stem Cells and Extracellular Vesicles in Vascular Tissue Regeneration. *ront Cardiovasc Med***5**, 86
35. Haraszti, R. A., Miller, R., Didiot, M. C., Biscans, A., Alterman, J. F., Hassler, M. R., Roux, L., Echeverria, D., Sapp, E., DiFiglia, M., Aronin, N., and Khvorova, A. (2018) Optimized Cholesterol-siRNA Chemistry Improves Productive Loading onto Extracellular Vesicles. *Mol Ther***26**, 1973-1982
36. Venereau, E., De Leo, F., Mezzapelle, R., Careccia, G., Musco, G., and Bianchi, M. E. (2016) HMGB1 as biomarker and drug target. *Pharmacol Res***111**, 534-544
37. Feng, Y., Ke, J., Cao, P., Deng, M., Li, J., Cai, H., Meng, Q., Li, Y., and Long, X. A.-O. (2018) HMGB1-induced angiogenesis in perforated disc cells of human temporomandibular joint. *J Cell Mol Med***22**, 1283-1291
38. Cheng, P., Ma, Y., Gao, Z., and Duan, L. (2018) High Mobility Group Box 1 (HMGB1) Predicts Invasion and Poor Prognosis of Glioblastoma Multiforme via Activating AKT Signaling in an Autocrine Pathway. *Med Sci Monit***24**
39. He, H., Wang, X., Chen, J., Sun, L., Sun, H., and Xie, K. (2019) High-Mobility Group Box 1 (HMGB1) Promotes Angiogenesis and Tumor Migration by Regulating Hypoxia-Inducible Factor 1 (HIF-1α) Expression via the Phosphatidylinositol 3-Kinase (PI3K)/AKT Signaling Pathway in Breast Cancer Cells. *Med Sci Monit***25**, 2352-2360

Figures

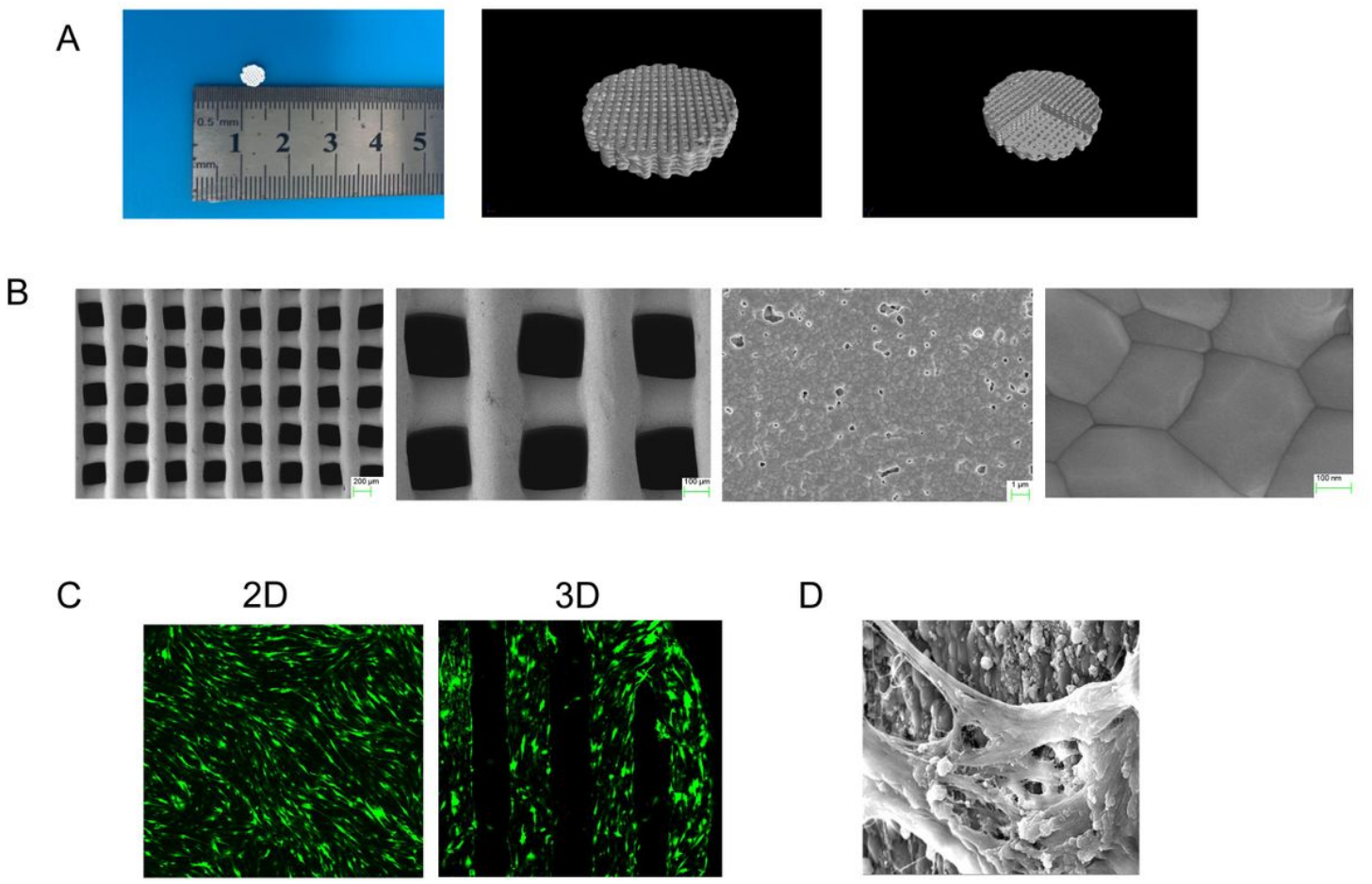

Figure 1

Characterization of 3D scaffoldand BMSC growth. (A). Representative micro-CT images of the 3D scaffold. (B). Morphology of 3D scaffold under transmission electron microscopy. (C). Confocal imaging of BMSCs in 2D culture and 3D scaffold by staining with calcein AM (live cells, green) and PI (dead cells, red). (D) Morphology of BMSCs in 3D scaffold detected by transmission electron microscopy.

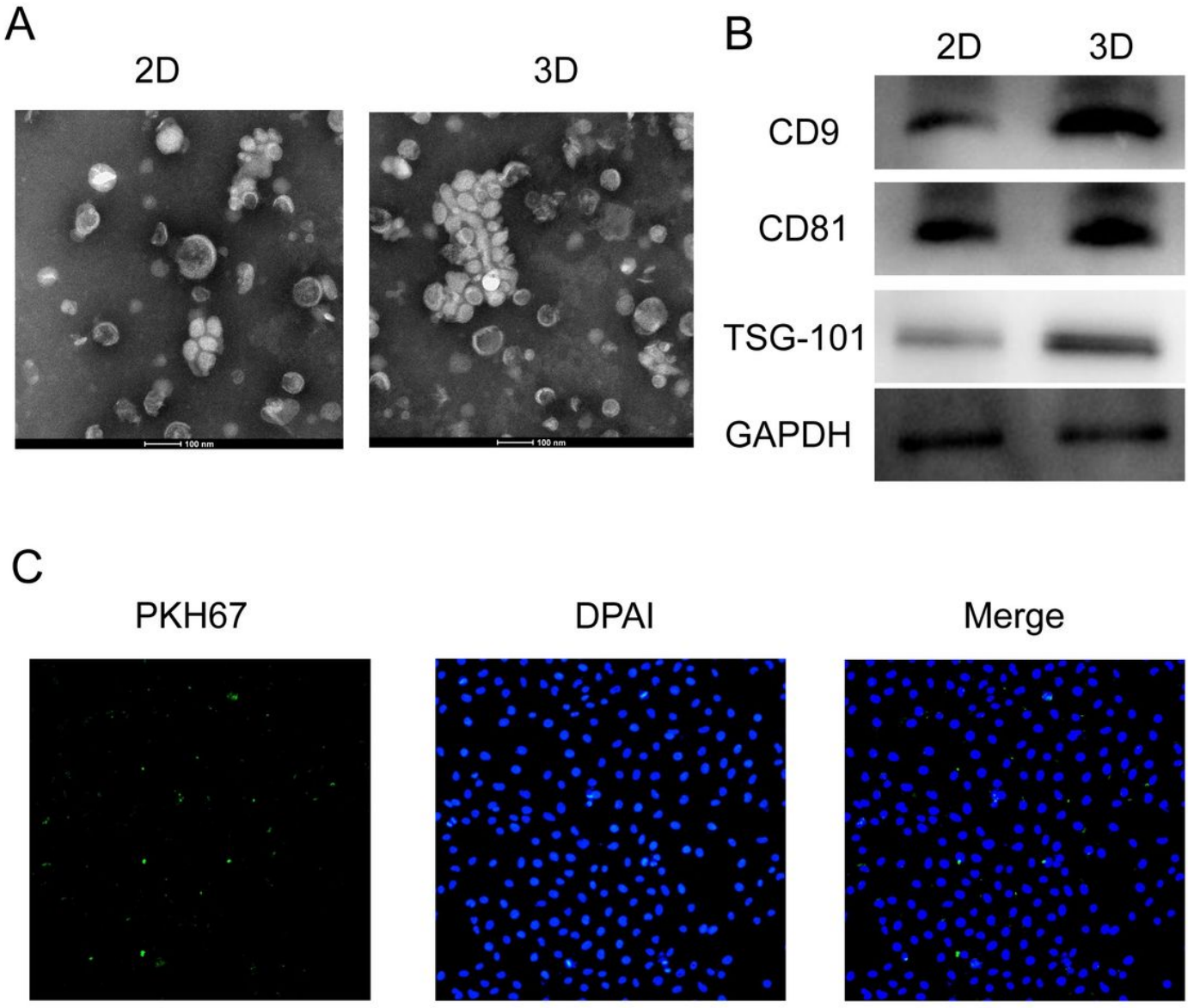

Figure 2

Characterization of 2D-exos and 3D-exos.(A). Morphology of 2D-exos (left) and 3D-exos (right) under transmission electron microscopy (scale bar 100 nm). (B). Western blot analysis of protein markers of exosomes in 2D or 3D culture. (C). Uptake of exosomes in HUVEC cells detected by confocal microscopy.

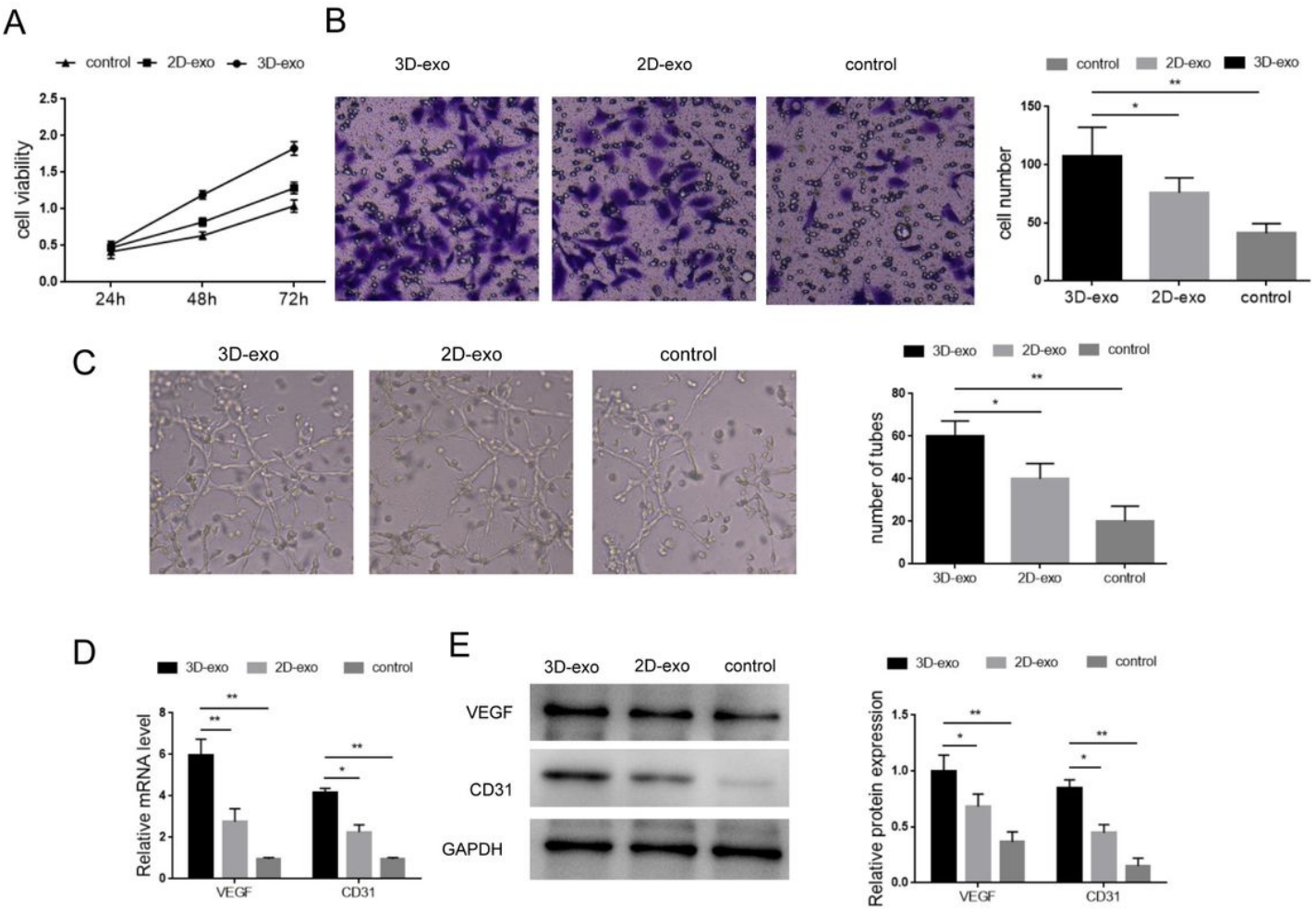

Figure 3

Effects of 2D-exos and 3D-exos on proliferation, migration and angiogenesis of HUVECs. (A). The proliferation of HUVECs was assessed by cck-8 assay. (B) Light microscopy images (left) and the number of transmitted HUVECs (right) in the Transwell migration assay. (C) Light microscopy images (left) and the number of tubes formed by HUVECs (right) in the tube formation assay. The protein (D) and mRNA level (E) of genes associated with angiogenesis (VEGF, CD31) detected by Western blotting. *p < 0.05, **p < 0.01, n = 3.

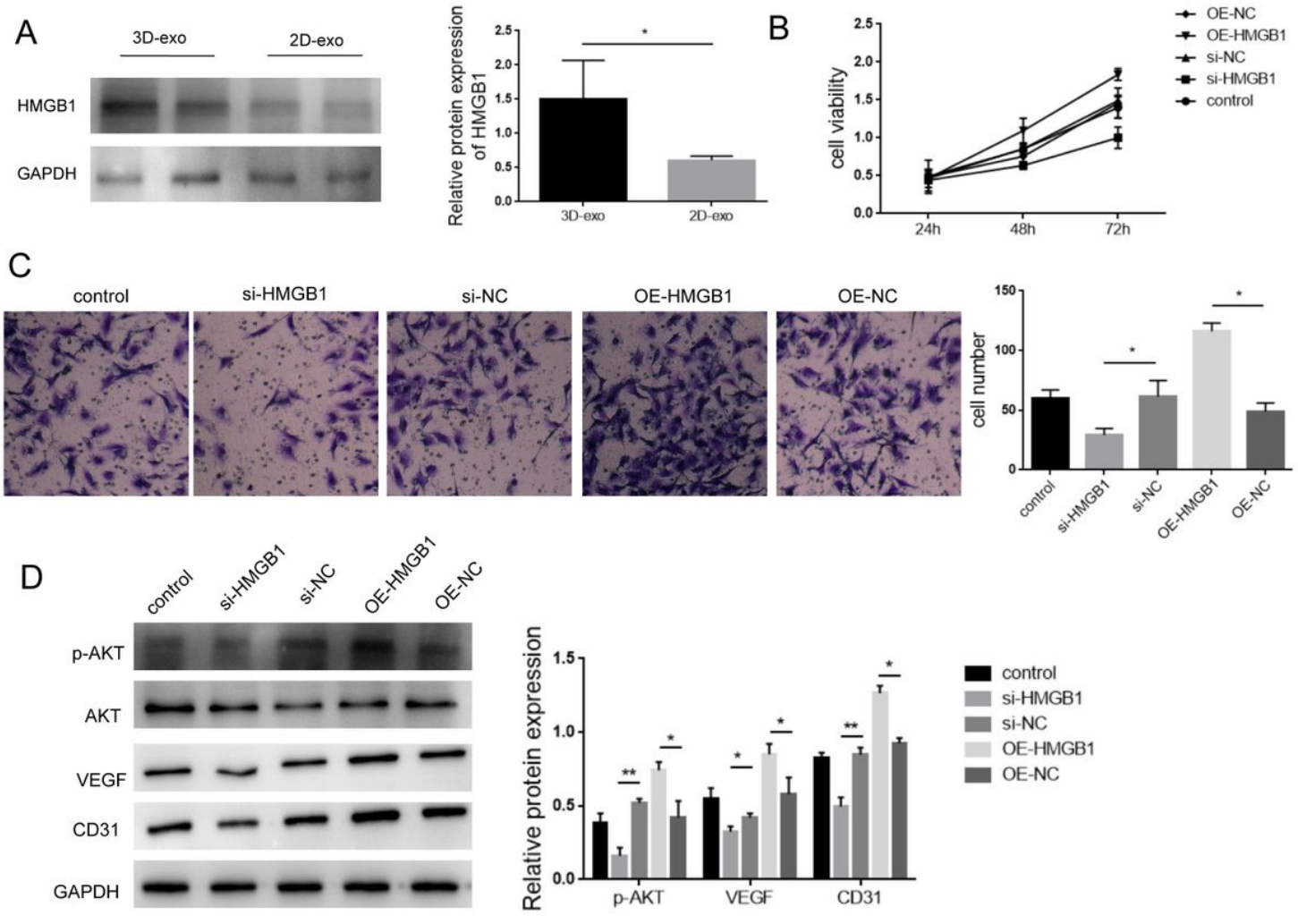

Figure 4

3D-exos modulate angiogenic through HMGB1 and AKT signaling pathway. (A) HMGB1 protein in HUVEC cells treated with 2D-exos or 3D-exos was detected by Western blotting. (B) The effect of 3D-exos on HUVEC proliferation was assessed by CCK-8 assay. (C) The effect of 3D-exos on migration was eliminated by transwell migration assay. (D)Western blot analysis of VEGF, CD31,AKT and p-AKT exposed to 2D-exos and 3D-exos. *p < 0.05, **p < 0.01, n = 3.

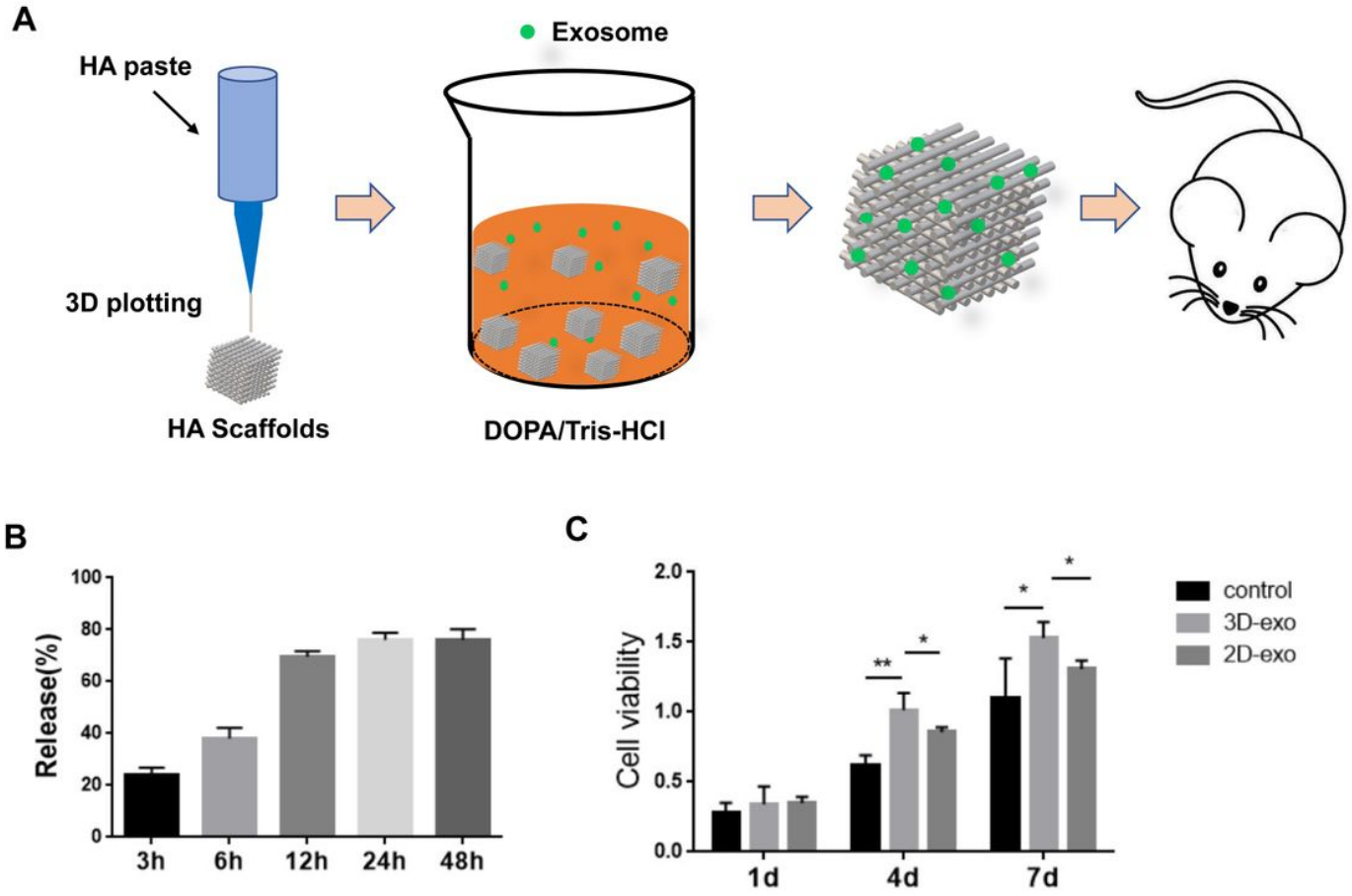

Figure 5

Incorporation of exosomes with hydroxyapatite scaffolds. (A) Schematic illustration of the preparation of 3D-Exo/hydroxyapatite (3D-Exo/HA) scaffolds. (B) The release rate of exosomes from HA scaffolds. (C) The effect of released exosomes on the proliferation HUVECs.

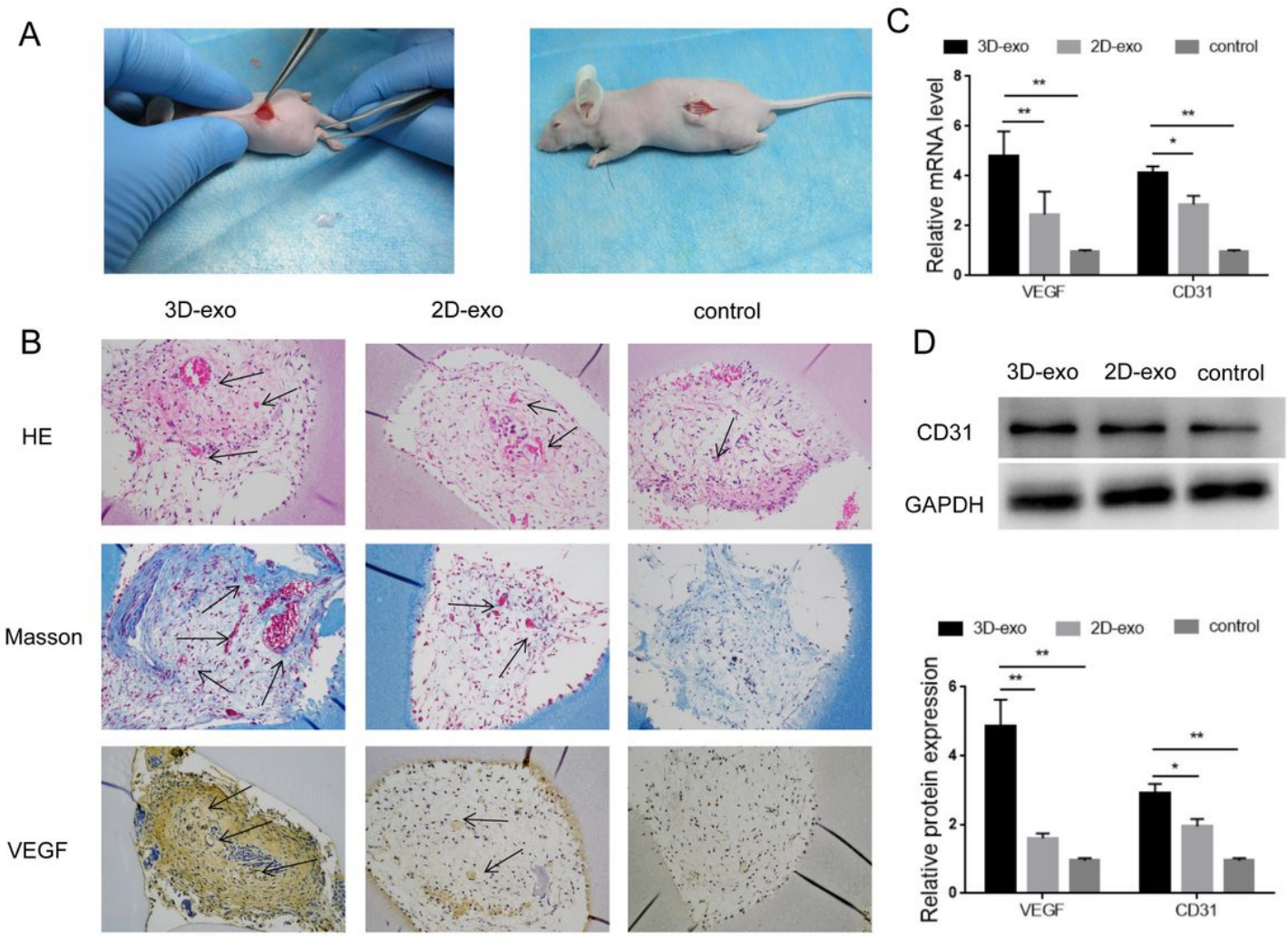

Figure 6

Effect of 2D-exos and 3D-exos on in vivo angiogenesis. (A) The models of in vivo angiogenesis were established. (B) HE, Masson, and immunohistochemical staining of scaffolds. The mRNA (C) and protein levels (D) of proteins associated with angiogenesis (VEGF, CD31). *p < 0.05, **p < 0.01, n = 3.

Supplementary Files

This is a list of supplementary files associated with this preprint. Click to download.

- FigureS1.tif